ELECTRON BEAM MOLECULAR LASERS

S. R. Byron

Mathematical Sciences Northwest, Incorporated

Prepared for:

Advanced Research Projects Agency
Office of Naval Research

August 1973

MSNW Report No. 74-105-2

MOLECULAR LASERS IN E-BEAM STABILIZED DISCHARGES

Semi-Annual Technical Report No. 2
Covering the Period
15 November 1972 to 15 May 1973

By

S. R. Byron, L. Y. Nelson, C. H. Fisher,
G. J. Mullaney, and A. L. Pindroh

Mathematical Sciences Northwest, Inc.
4545 Fifteenth Avenue N. E.
Seattle, Washington 98105

August 1973

Contract N00014-72-C-0430

Sponsored by

Advanced Research Projects Agency
ARPA Order No. 1807

Monitored by

Office of Naval Research
Code 421

ARPA ORDER NO.:	1807
PROGRAM CODE:	2E90
NAME OF CONTRACTOR:	Mathematical Sciences Northwest, Inc.
EFFECTIVE DATE OF CONTRACT:	15 March 1972 to 15 November 1973
CONTRACT AMOUNT:	$437,935
CONTRACT NUMBER:	N00014-72-C-0430
PRINCIPAL INVESTIGATOR:	Dr. S. R. Byron (206)524-9300
SCIENTIFIC OFFICER:	Director, Physics Programs Physical Sciences Division Office of Naval Research Department of the Navy 800 North Quincy Street Arlington, Virginia 22217
DISCLAIMER:	The views and conclusions contained in this document are those of the authors and should not be interpreted as necessarily representing the official policies, either expressed or implied, of the Advanced Research Projects Agency or the U. S. Government.

ABSTRACT

This program is directed toward developing efficient, high energy density electric discharge lasers in the infrared and visible regions of the spectrum. A high current, electron-beam-stabilized, electric discharge is used for excitation. Infrared laser emission and absorption from the vibrational levels of HF (2.8 to 3.1 μm) and DF (3.8 to 4.1 μm) in various gas mixtures is being studied to determine laser efficiency and to obtain a detailed model of the vibrational kinetics. The efficiency of electric discharge excitation of molecular vibration in these gases is being determined by solving the electron Boltzmann equation. Electronic state excitation by e-beam stabilized electric discharges in N_2 and other molecular systems is being investigated in an effort to develop efficient, long pulse visible lasers.

TABLE OF CONTENTS

LIST OF TABLES

LIST OF FIGURES

SECTION I

SUMMARY

A high current electron-beam-stabilized electric discharge chamber has been constructed and used successfully to achieve laser action at 2.8 to 3.1 μm in $Ar/H_2/HF$, Ar/HF, $Ar/N_2/HF$, and N_2/HF gas mixtures. Laser emission was observed on the 1-0, 2-1, and 3-2 P-branch transitions in gas mixtures containing 0.2 to 0.5 percent HF. The electric discharge chamber was constructed with a half-meter optical gain path, which minimized the threshold gain required. The plasma diode supplied an electron beam current density of about 40 ma/cm^2 which provided sufficient discharge power input at a low enough E/N ($\leq 1 \times 10^{-16}$ $V\text{-}cm^2$) to prevent H_2 dissociation by the discharge.

The Boltzmann equation for the electron energy distribution function was solved to determine the fractional power transfer into the various internal energy modes of H_2 in a 90/10 argon/hydrogen mixture. Rotational heating was found to absorb a significant portion ($\sim$ 30 percent) of the input power at an E/N of 0.5×10^{-16} $V\text{-}cm^2$; dissociation becomes a serious problem at an E/N above 1×10^{-16} $V\text{-}cm^2$.

It was found experimentally that the performance of a pin-discharge N_2 ($B^3\pi_g \rightarrow A^3\Sigma_u^+$) infrared laser improves with the addition of small amounts (1 percent) of SF_6, or other gases with large electron attachment cross sections. Calculations carried out for triplet state energy pooling of

the $N_2(A)$ state indicate that this may be a viable means for producing a long pulse, high energy N_2 visible laser.

SECTION II

PLASMA DIODE ELECTRON GUN AND ELECTRIC DISCHARGE CHAMBER

Earlier measurements of HF fluorescence in $Ar/H_2/HF$ discharges, combined with analytical modeling (Ref. 1), indicated that higher electron beam current density and a longer optical path were needed to achieve laser threshold conditions. The electron gun used for this purpose is a plasma diode; a low pressure, high voltage glow discharge of the type that has been described recently by O'Brien (Ref. 2). The configuration used here is shown schematically in Figure 1. A 7.6-cm inside diameter glass envelope was fitted with a solid, polished aluminum cathode and a 60 percent transmitting anode screen. A 1.25-cm radius of curvature edge on the cathode was used to reduce field concentrations and minimize glow-to-arc transition at high voltage. After evacuating and outgassing the diode, helium at pressures of 50 to 100 microns was admitted. A stable, high voltage glow discharge was produced in the tube which provided an internal electron beam current density of up to 0.5 amps/cm^2 at a voltage up to 125 kV.

While the sensitivity to contamination is far less critical than for thermionic cathode electron guns, good vacuum technique and care in selection of materials for low degassing rates are important for successful operation of the device at high voltage. The plasma diode components were degreased, cleaned in an ultrasonic bath first with

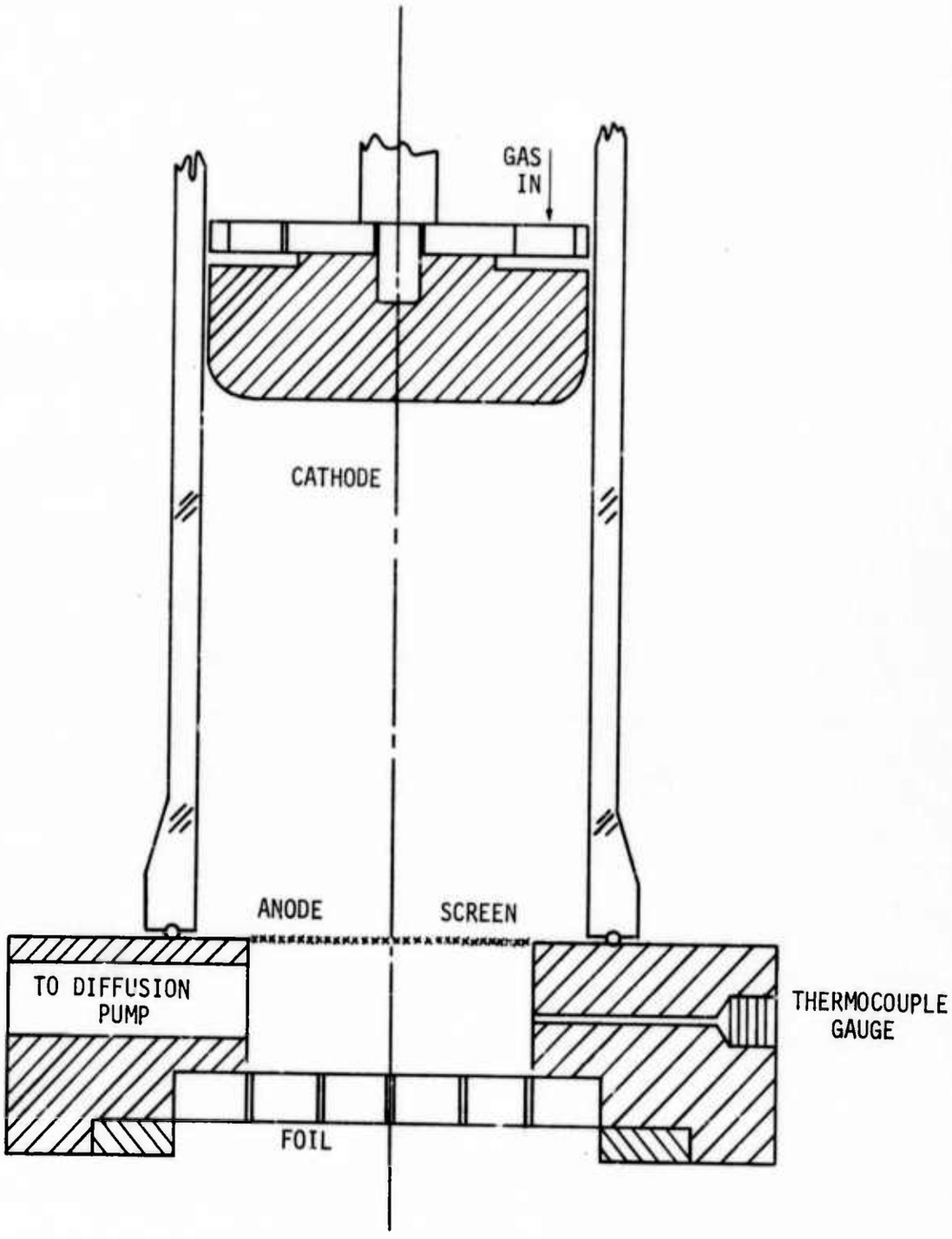

Figure 1. Schematic of Plasma Diode. Discharge Diameter, 7.6 cm; Side Walls Glass; Cathode Aluminum; Anode Screen Stainless Steel; Foil 0.025 mm Aluminum or 0.012 mm Titanium; Anode-Cathode Spacing 10 cm; Fill Gas He 50-100 μm.

acetone then with methanol, and dried with a heat gun. The single tube device of Figure 1 (about 0.5 liter volume) would typically have a leak and/or outgassing rate of less than 0.1 micron per minute. During operation, helium was admitted steadily to the top of the diode chamber and pumped from a port below the anode screen. A small helium flow rate (about 25 microns per minute) was used to assure that impurities would be negligible compared to the helium concentration.

It was found that a conditioning process was required to eliminate glow to arc transition during pulsed operation at high voltage. Starting at low pressure (less than 50 μ of helium), the voltage and pressure were gradually raised until a glow discharge could be obtained reliably without arcing. Several hundred pulses were required to eliminate glow to arc transition at high voltage. Once conditioned, the plasma diode ran in the glow discharge mode with excellent repeatability in its operating characteristics.

Typical performance of the plasma diode is shown in Figures 2 and 3. The maximum diode voltage was 125 KV without arcing. The maximum current density through a 0.0012-cm titanium foil at the center of the diode was 150 ma/cm^2. The diode was generally operated under conditions which provided an average current density of 50 ma/cm^2 for a time interval of about 30 μsec.

The successful operation of the single plasma diode electron gun led to the design and construction of a 5- x 50-cm apparatus utilizing the plasma diode electron beam to stabilize the electrical

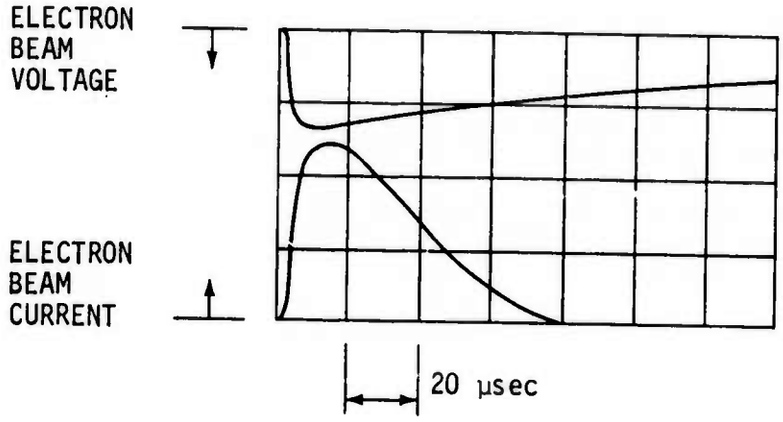

Figure 2. Typical Electron Beam Voltage and Current Versus Time; Peak Electron Beam Voltage 110 KV; Peak Electron Beam Current Density 100 ma/cm^2 Measured 2 cm from the 0.012 mm Thick Titanium Foil; Helium Pressure was 95 Microns.

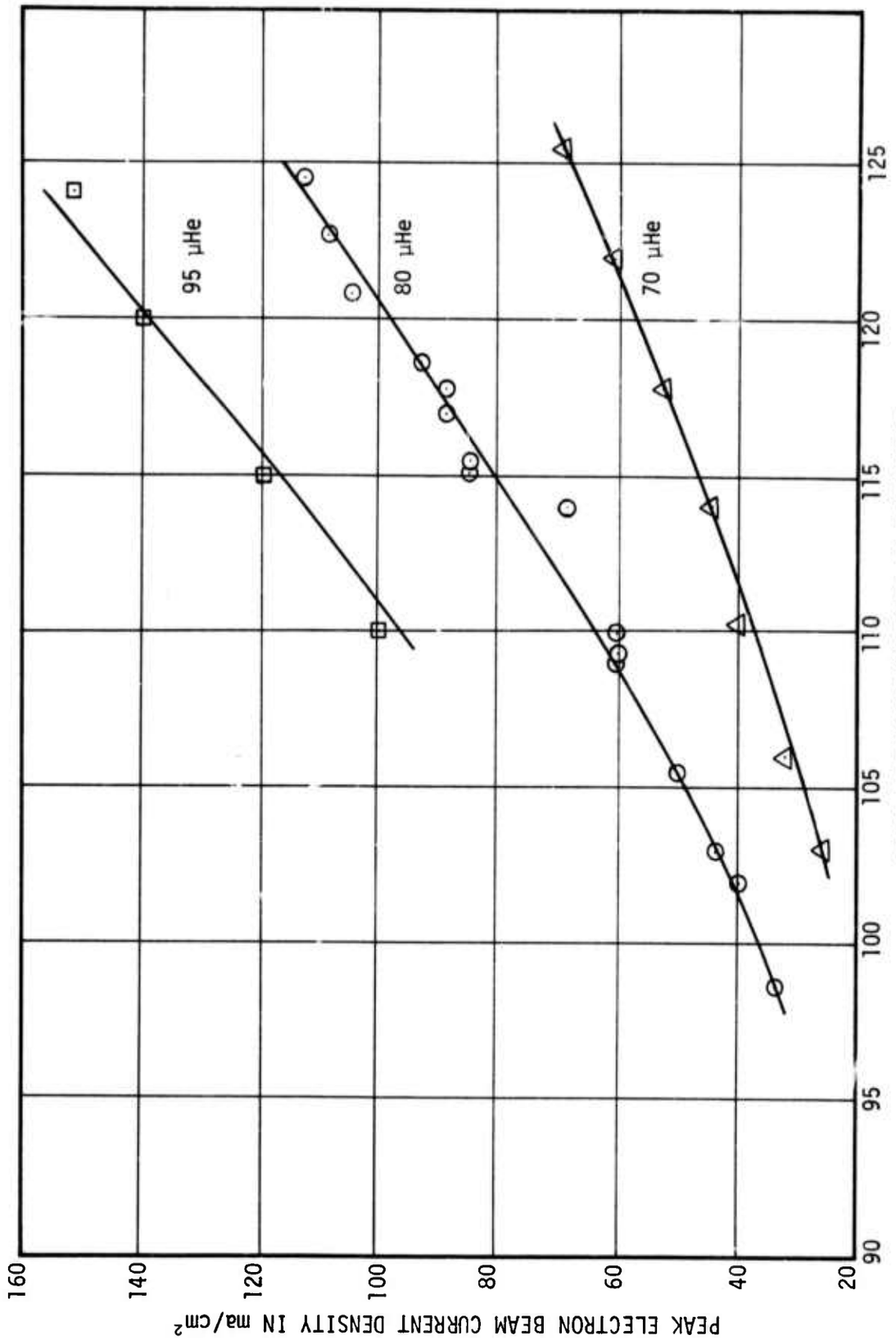

Figure 3. Peak Electron Beam Current Density at a Distance 2 cm from a 0.012 mm Thick Titanium Foil

discharge. The most expeditious approach to building the larger system was to use the unit already developed as a module and place five cylindrical units side-by-side on a common base (Figure 4). This led to a minimum development time before proceeding with our laser objectives. However, with this geometry, a certain amount of beam nonuniformity had to be accepted.

A block diagram of the electrical system built for the five tube plasma diode and the electrical discharge cell is shown in Figure 5. The Marx bank trigger received an input signal from the gate output of an oscilloscope and was fired without a delay. The effective capacitance of the Marx bank was 0.1 μf. The same oscilloscope gate output fired both the electrical discharge bank (100 μf capacitor) and the electrical discharge dump through variable time delays.

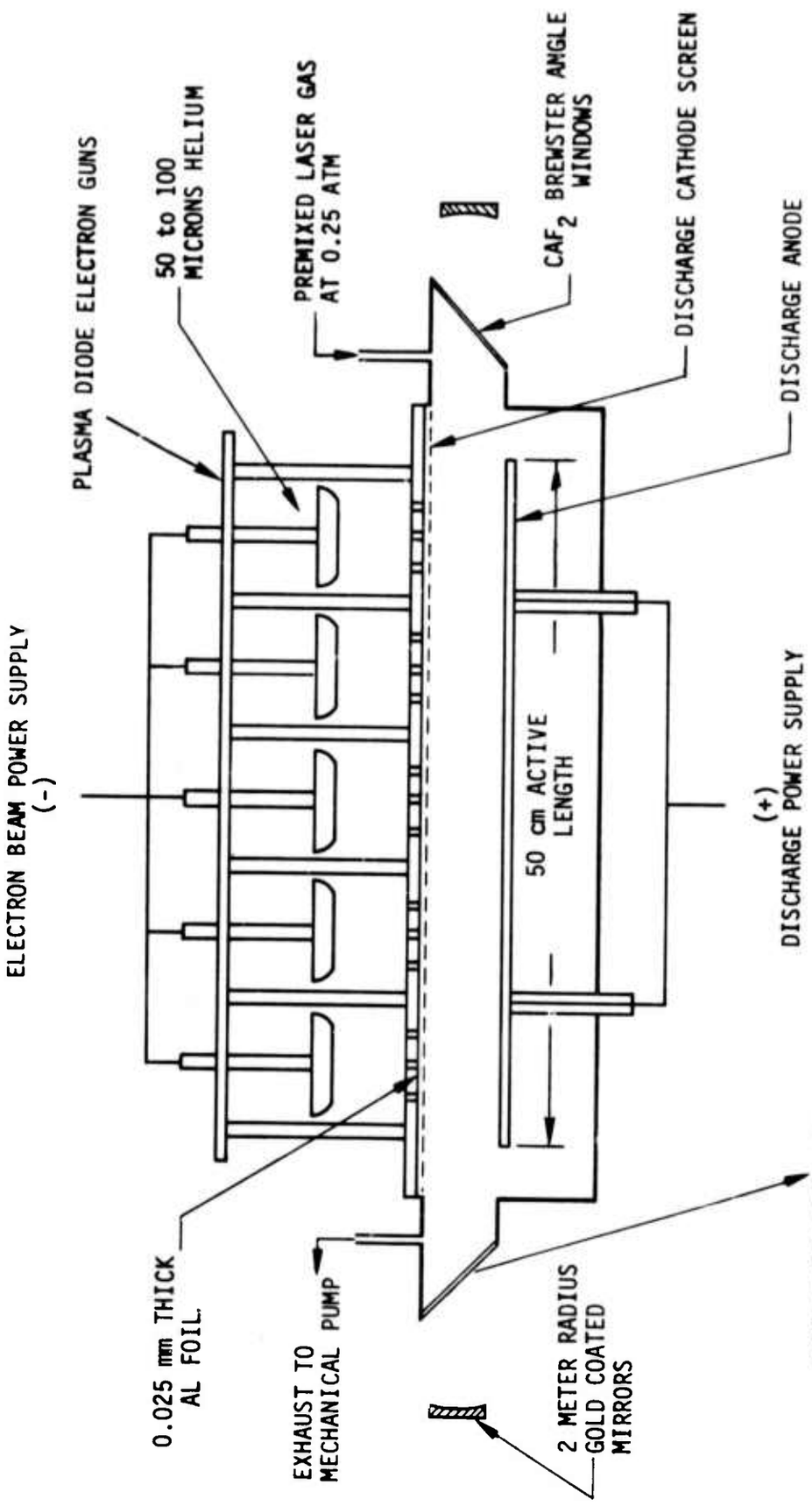

Figure 4. Schematic of Plasma Diode Electron-Beam-Stabilized Electric Discharge Cell and Laser Cavity

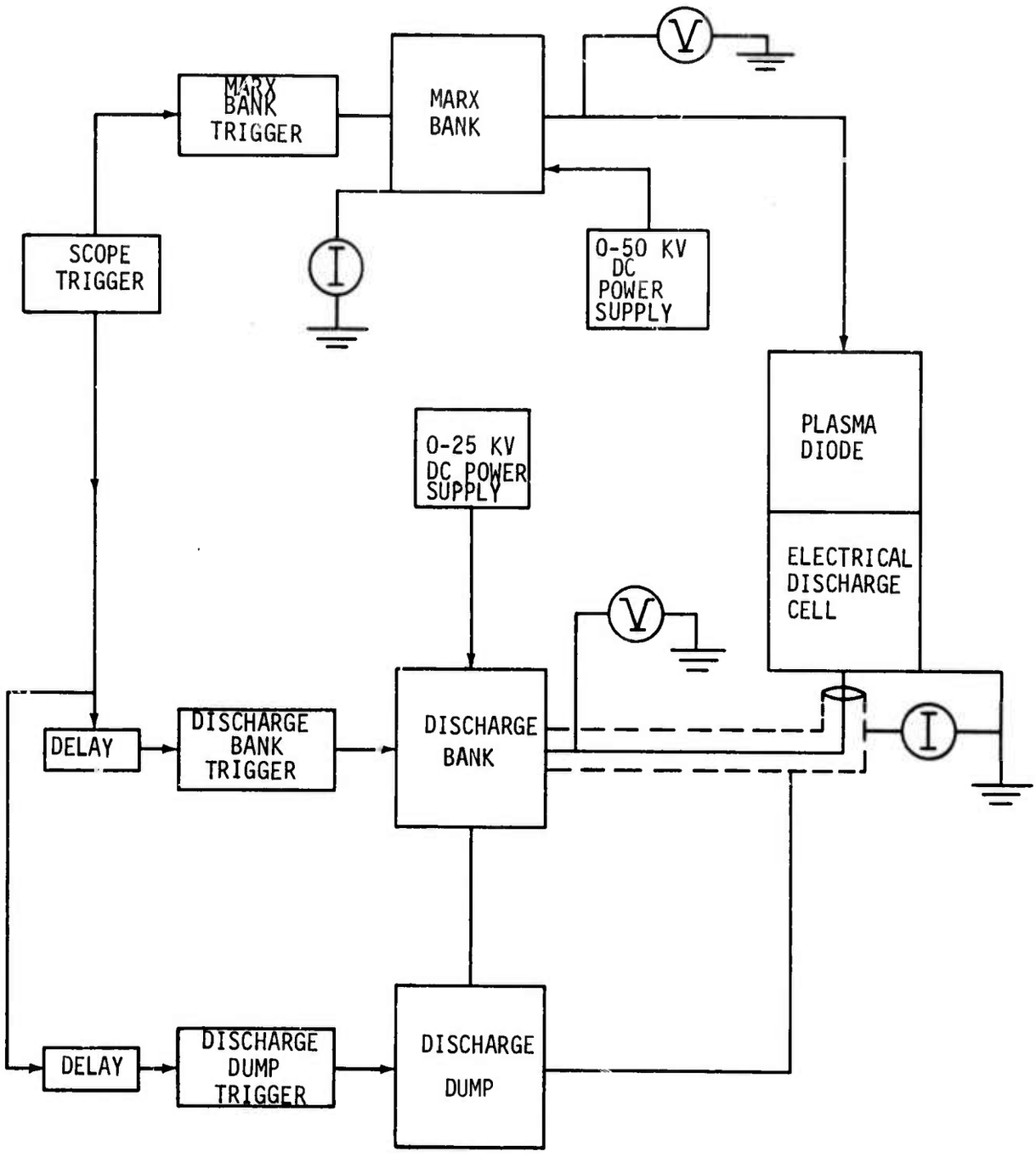

Figure 5. Block Diagram of the Electric Circuitry Used with the Plasma Diode Electron-Gun and Electrical Discharge Cell

SECTION III

HF ELECTRIC DISCHARGE LASER EXPERIMENTS

The electron beam apparatus shown in Figure 4 contains a discharge cell equipped with CaF_2 Brewster angle windows and 2-m-radius gold coated mirrors to form a high-Q optical cavity. The internal cavity intensity was sampled by recording light scattered by one of the CaF_2 windows onto a liquid nitrogen cooled Ge:Au detector. Laser emission was tested by observing a change in intensity of more than 3 orders of magnitude when the cavity mirror furthest from the detector was blocked. The spectral output was determined by using a 1/4-m Jarrell-Ash monochromator with a spectral resolution of 0.002 μm. A means for optimizing the laser cavity mirror alignment, at the HF laser wavelengths, was found using chemical laser emission from a mixture of $Ar/H_2/SF_6$. This mixture will lase for a time duration of about 50 μsec using the electron beam alone to dissociate SF_6 and produce vibrationally excited HF by chemical reaction. Following the mirror alignment procedure laser emission was observed in $Ar/H_2/HF$ mixtures by V-V pumping using an e-beam sustained electric discharge to vibrationally excite H_2. Laser emission was also produced in $Ar/N_2/HF$, N_2/HF, and Ar/HF mixtures. In the following section the dependence of HF laser emission on gas mixtures and discharge parameters will be discussed along with the laser wavelengths observed and possible mechanisms responsible for these observations.

3.1. $Ar/H_2/SF_6$ and $Ar/D_2/SF_6$ Chemical Laser Emission

Dissociative electron attachment of lower energy electrons in SF_6 is an effective way of producing F atoms for the chemical laser reaction $F + H_2 \rightarrow HF\dagger + H$. Hence our electron beam source is sufficient to produce HF laser emission in an SF_6/H_2 mixture, without the use of an applied electric field. We have found that mixtures of 80/10/10 ($Ar/H_2/SF_6$) at 200 torr total pressure completely remove the free electrons produced by the electron beam, and essentially no discharge current can be drawn when an electric field is applied. An $Ar/D_2/SF_6$ mixture readily produced DF laser action as well. The chemical laser output lasted about 50 μsec, corresponding to the duration of significant electron beam current through the foil. Detailed measurements of spectral output were not necessary at this point and have been postponed until the more important tests using $Ar/H_2/HF$ mixtures were completed. Cavity mirror alignment was optimized using SF_6/H_2, by maximizing the intracavity laser intensity measured by the Ge:Au detector (Figure 4).

3.2. $Ar/H_2/HF$, and Ar/HF Electric Discharge Laser Emission

In accord with earlier predictions (Ref. 1), gas mixtures containing predominantly argon, 10 - 20 percent H_2, and less than 1 percent HF were found to produce HF laser emission at 2.8 μm to 3.1 μm. The total gas pressure was 200 torr. A slow gas flow was maintained to clear out the discharge chamber between pulses.

The added HF (0.2 to 0.5 percent) had no measurable effect on the electric discharge current, indicating that dissociative attachment to HF was smaller than dissociative recombination of molecular ions under these conditions. The applied electric field (E/N) ranged from values of 0.3×10^{-16} to 0.5×10^{-16} V-cm^2 and resulted in peak electrical discharge currents of 8 to 10 A/cm^2. The electrode spacing was 3 cm and the anode was 5 cm wide by 48 cm long.

The laser lines observed in various gas mixtures are shown in Table I. Only P-branch lines were seen. The times given in Table I are referred to the start of the electrical discharge pulse in the laser gas and represent the time of onset and the time of termination of laser emission for a single set of operating conditions in each gas mixture.

In Table I it is seen that laser emission often occurs simultaneously on more than one rotational line of a particular vibration band. This indicates a partial lack of rotational equilibration, although the continuing shift from lower to higher J values throughout the pulse duration indicates a tendency toward rotational equilibration with the rising gas temperature. This effect is similar to that observed in pulsed HF chemical lasers by Suchard (Ref. 3). It is also seen in Table I that there is considerable correlation between laser emission on $P_v(J)$ and emission on $P_{v-1}(J+1)$, indicating significant cascade coupling.

The results obtained in pure argon with HF [Fig. 6(a)] demonstrate that direct electron impact excitation of vibration of HF is

effective in producing a partial inversion in the low vibrational levels of HF at room temperature. For this mixture the optimum E/N was about 0.1×10^{-16} V-cm^2 and the electrical discharge current density was about 4 A/cm^2. Higher values of E/N could not be used in Ar/HF mixtures due to early formation of an unstable electrical discharge. Higher HF concentrations than 0.5 percent led to little or no laser emission because of the rapid V-R,T decay rate of HF.

Table I

Time-Resolved Spectroscopic Measurements of the Vibration-Rotation Lines Observed in an HF Electric Discharge Laser
(Gas Pressure, 200 Torr; Time in μsec)

Transition Band	P(J)	Wavelength(μm) HF	Gas Mixture Ar/HF	Ar/H_2/HF	Ar/N_2/HF	N_2/HF
1-0	9	2.823	...	...	(25 - 57)	...
2-1	7	2.870	(10-32)	...	(6 - 44)	(12-28)
2-1	8	2.911	(12-40)	(8 - 22)	(8 - 66)	
2-1	9	2.954	...	(11 - 32)	...	...
2-1	10	2.999	...	(22 - 38)	...	...
3-2	6	2.964	(9-13)	...	(6 - 9)	...
3-2	7	3.005	(10-28)	(10 - 18)	(7 - 45)	...
3-2	8	3.048	...	(10 - 27)	(32 - 48)	...
3-2	9	3.094	...	(24 - 32)	...	...

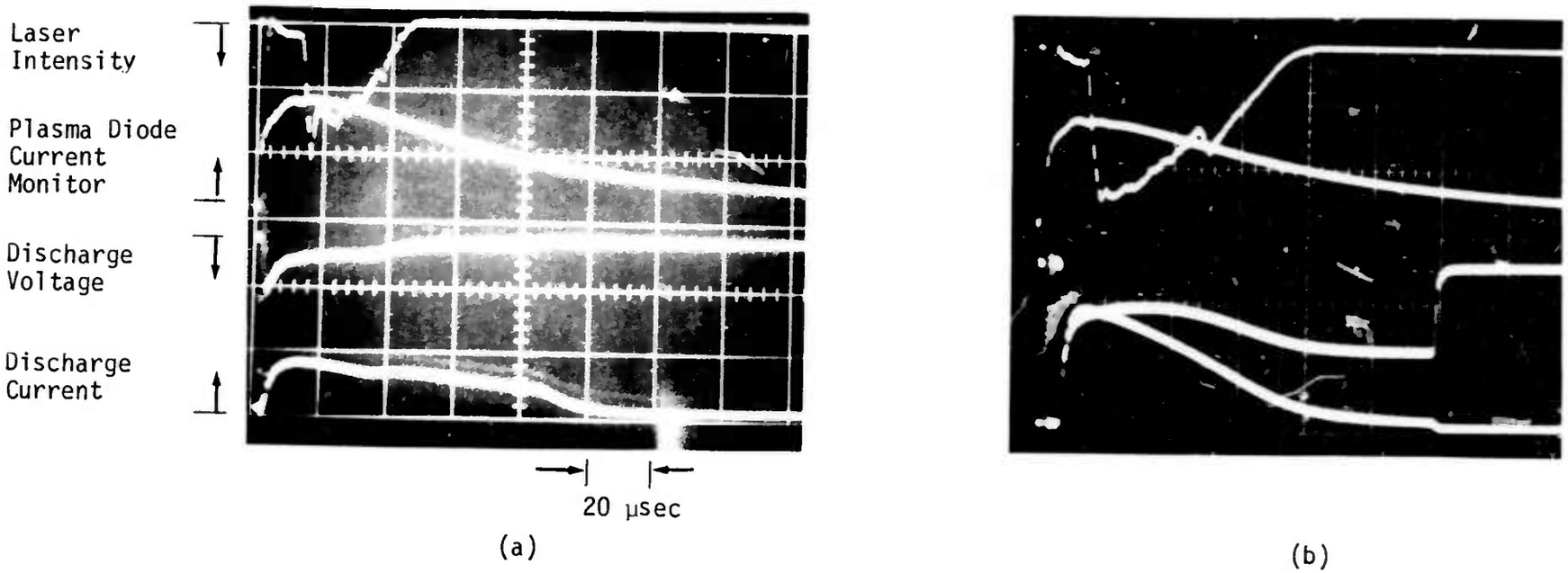

Figure 6. Electric Discharge Excitation of HF Laser Emission in Mixtures of (a) 0.99 Ar and 0.004 HF, and (b) 0.89 Ar, 0.10 N_2, and 0.004 HF. The Discharge Voltage Sensitivity is 700 V/Div and the Discharge Current Sensitivity is 1380 A/Div.

The maximum laser output obtained using argon plus 10% H_2 with HF (Fig. 7(a)) was substantially higher than the maximum obtained using argon plus 10 percent D_2 with HF (Fig. 7(b)). This is taken as strong evidence for vibrational transfer from H_2 to HF. Probe laser measurements of the decay rate of the HF vibrational levels are needed to establish the H_2 V-V pumping mechanism and kinetics.

3.3. $Ar/N_2/HF$, and N_2/HF Laser Emission

While searching for the superfluorescent spiking of the first and second positive systems of N_2 previously observed in $Ar/N_2/HF$ mixtures, HF infrared laser emission was obtained. The lines observed are presented in Table I. Quite surprisingly, a 1-0 line was observed, which indicates a high vibrational temperature among the lowest vibrational states of HF. In Figure 8 the inversion necessary to achieve gain on 1-0 P(9) rather than P(8) or P(10) is shown at various temperatures. Assuming only slight heating by the discharge, N_1/N_0 must be approximately 0.2 to 0.25 for the gain to exceed cavity losses.

Gas mixtures were typically 90/10 Ar/N_2 with 0.2 - 0.5 percent HF producing optimum output at an E/N of 0.5×10^{-16} V-cm^2 and discharge currents of 10 A/cm^2. In the absence of Ar, output was quite low: typical values of E/N were 0.5×10^{-16} - 0.9×10^{-16} V-cm^2 and discharge currents ranged from 4 to 6 A/cm^2.

The pumping mechanism operating in the N_2 gas mixtures is not known at this time. There are two likely possibilities: (1) two

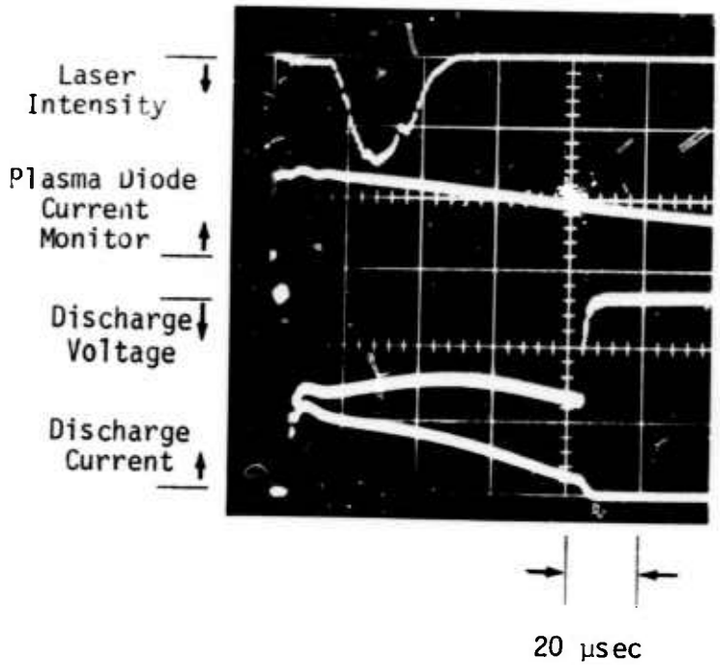

(a)

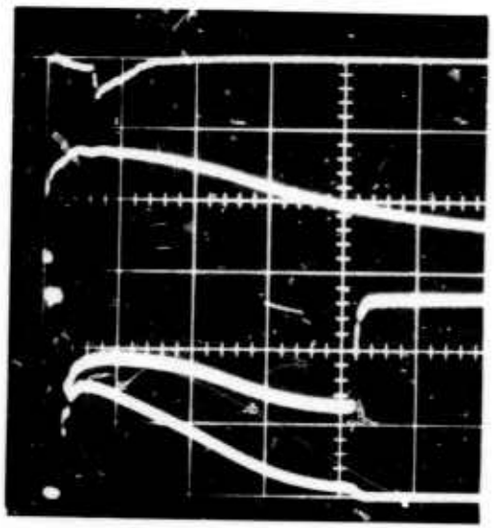

(b)

Figure 7. Electric Discharge Excitation of HF Laser Emission in Mixtures of (a) 0.89 Ar, 0.10 H_2, and 0.004 HF, and (b) 0.89 Ar, 0.10 D_2, and 0.004 HF. Voltage and Current Sensitivities Same as in Figure 6.

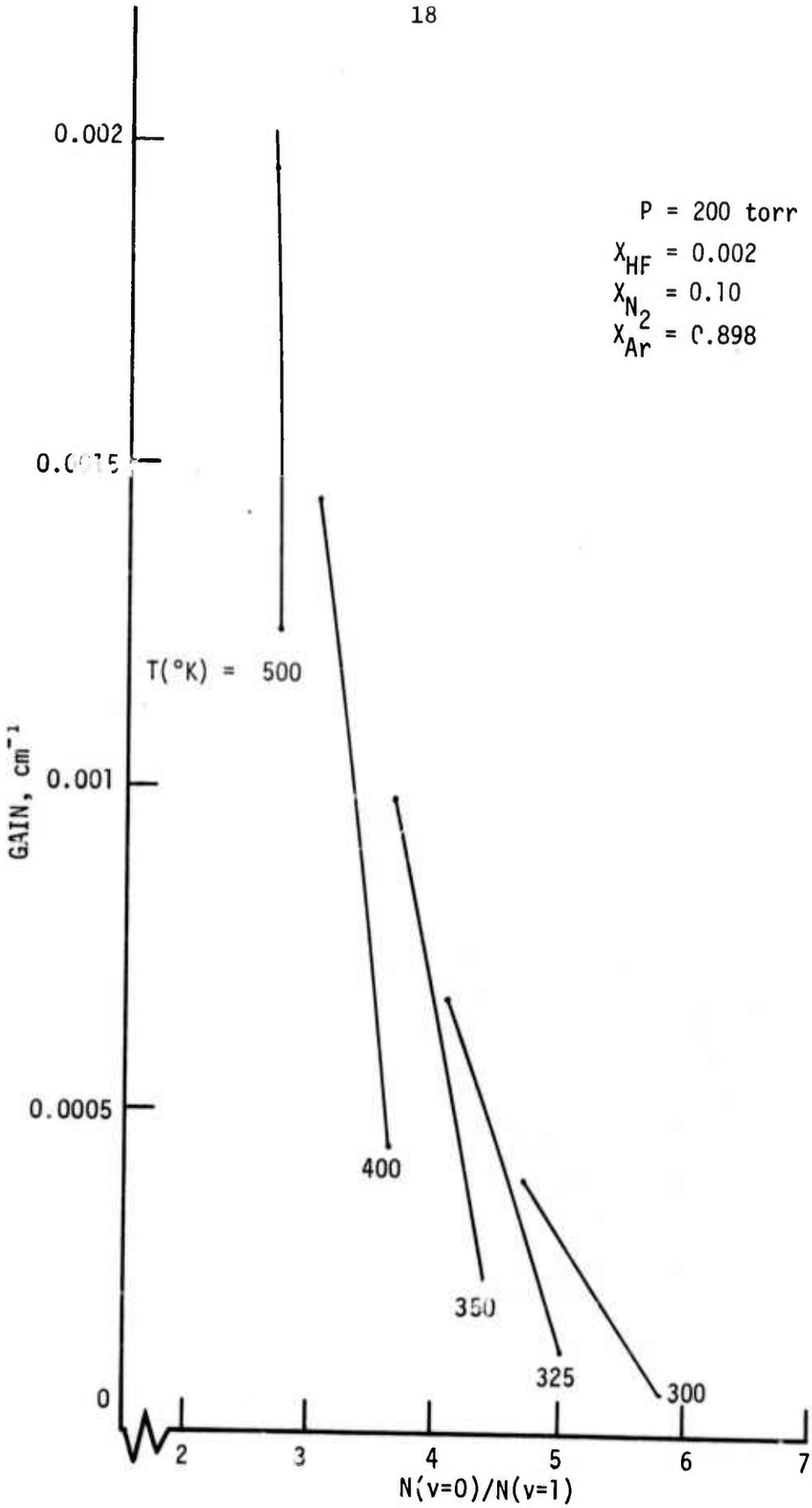

Figure 8. Range of Population Ratios for V = 1 → 0 Gain to be at a Maximum on P(9)

quantum V-V transfer from vibrationally excited N_2 to HF; (2) direct electron impact excitation of HF, with the N_2 serving to create a favorable electron energy distribution in the discharge. A probe laser measurement of the HF vibrational decay time following the discharge crowbar is planned in order to identify any long term V-V pumping mechanism from N_2 to HF.

3.4. Ar/D_2/DF Laser Search

Attempts to lase DF have thus far been unsuccessful. The inherent gain per molecule of DF is lower than that of HF (smaller Einstein A coefficient and smaller rotational constant). Thus the inversion in D_2 achieved by the electric discharge must be better than that in H_2. Deactivation rates of common atmospheric impurities (N_2, O_2) are approximately a factor of ten faster for DF than for HF; therefore, impurities will be a greater problem in DF gas mixtures. Higher purity DF and D_2 gases will be purchased for future work and purification methods will also be improved.

SECTION IV

SOLUTION TO THE BOLTZMANN EQUATION FOR Ar/H_2 MIXTURES

The energy partition between rotation, vibration, and electronic excitation in electric discharges in argon-hydrogen mixtures has been studied analytically using the best currently available experimental data for electron impact cross sections. The electric discharge is assumed to be stabilized at any desired value of E/N by the use of an external volume ionizing source such as a high voltage electron beam.

The analytical model development was divided into the following two parts:

1. Determination of elastic and inelastic electron impact cross sections for H_2 and Ar.
2. Solution of the Boltzmann equation to obtain the electron energy distribution function in H_2-Ar mixtures at various values of E/N.

Each of these is discussed below.

4.1. Elastic and Inelastic Cross Sections

The momentum transfer cross sections for electron impact on H_2 and Ar are shown in Figure 9. The dashed curve for H_2 was used by Engelhardt and Phelps (Ref. 4) in an earlier study of transport coefficients in H_2-Ar mixtures. The solid curve for H_2 was derived from recent electron beam measurements in H_2 by Linder and Schmidt (Ref. 5) and is currently being used in our computer program.

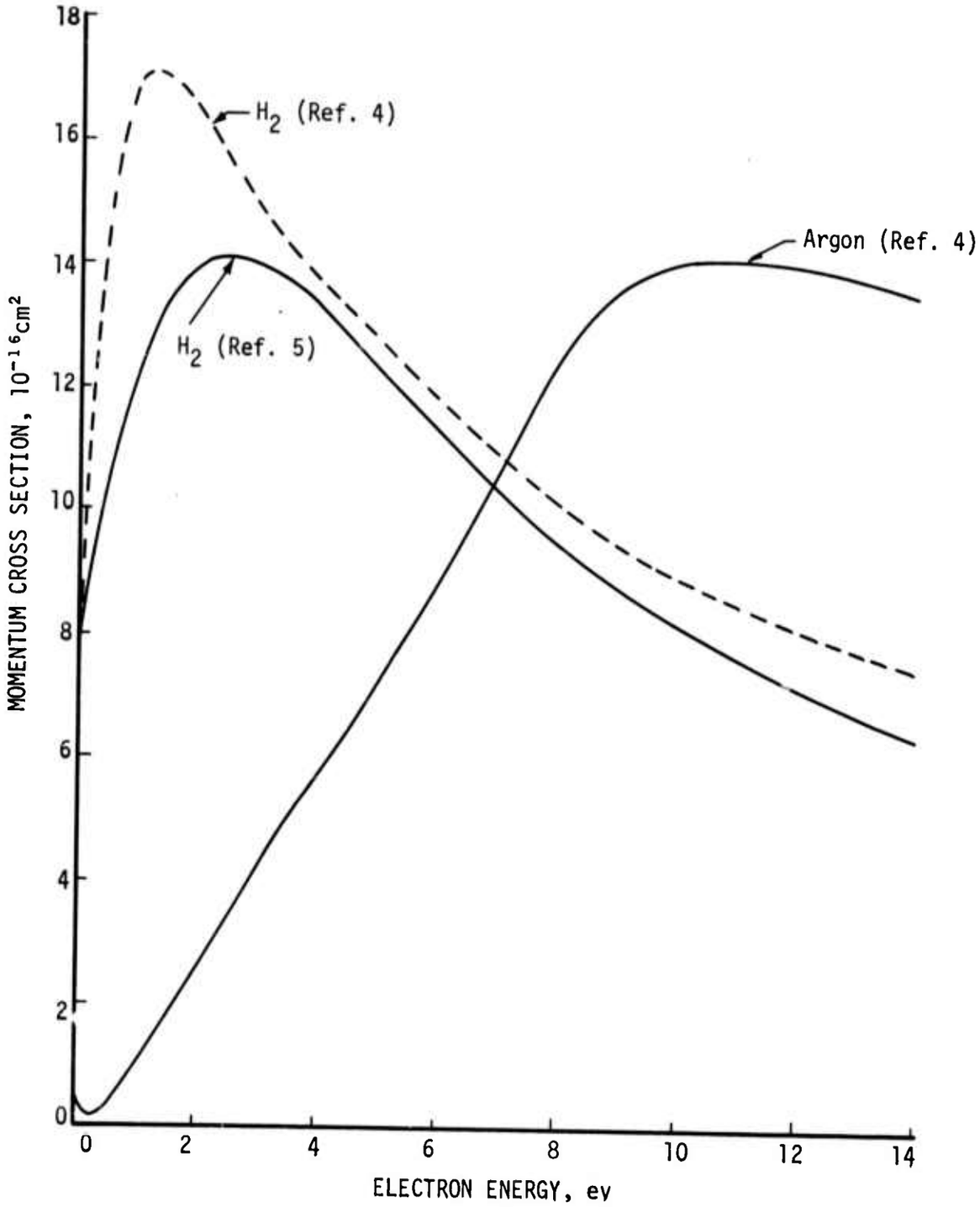

Figure 9. Momentum Transfer Cross Sections for H_2 and Argon

The inelastic cross sections for H_2 and Ar are shown in Figure 10. The total rotational excitation cross section of H_2, obtained from Linder and Schmidt (Ref. 5) is for a $j = 1 \rightarrow j = 3$ transition. This is satisfactory at room temperature since most of the H_2 is in the $j = 1$ state. The value of this cross section is an order of magnitude larger than that used by Engelhardt and Phelps (Ref. 4). The vibrational excitation cross section of H_2 is for the $v = 1$ state; the cross section for excitation of $v = 2$ is believed to be an order of magnitude smaller than that for $v = 1$ and is currently being neglected since no experimental data have been found. The electronic excitation cross section of H_2 is for the process $X^1\Sigma_g^+ \rightarrow b^3\Sigma_u^+$ which leads to dissociation of H_2. A characteristic electron energy loss of 10 ev is assumed. Also shown are cross sections for excitation of upper electronic states of H_2 which lead to uv emission and for direct ionization of H_2, both from Engelhardt and Phelps (Ref. 6).

The inelastic cross sections for H_2 described above have been used together with a computer program that solves the Boltzmann equation to determine electron transport properties in pure H_2. The resulting values of characteristic energy, $\varepsilon_k = eED/v$, agree satisfactorily with experimental data (Ref. 6), but computed values of the drift velocity, v, are too high by 10% to 40%, as shown in Figure 11. Thus completely satisfactory values of the cross sections of H_2 have not yet been found and work on this problem is continuing.

The inelastic cross section for electronic excitation plus ionization of argon is taken from Englehardt and Phelps (Ref. 4). A

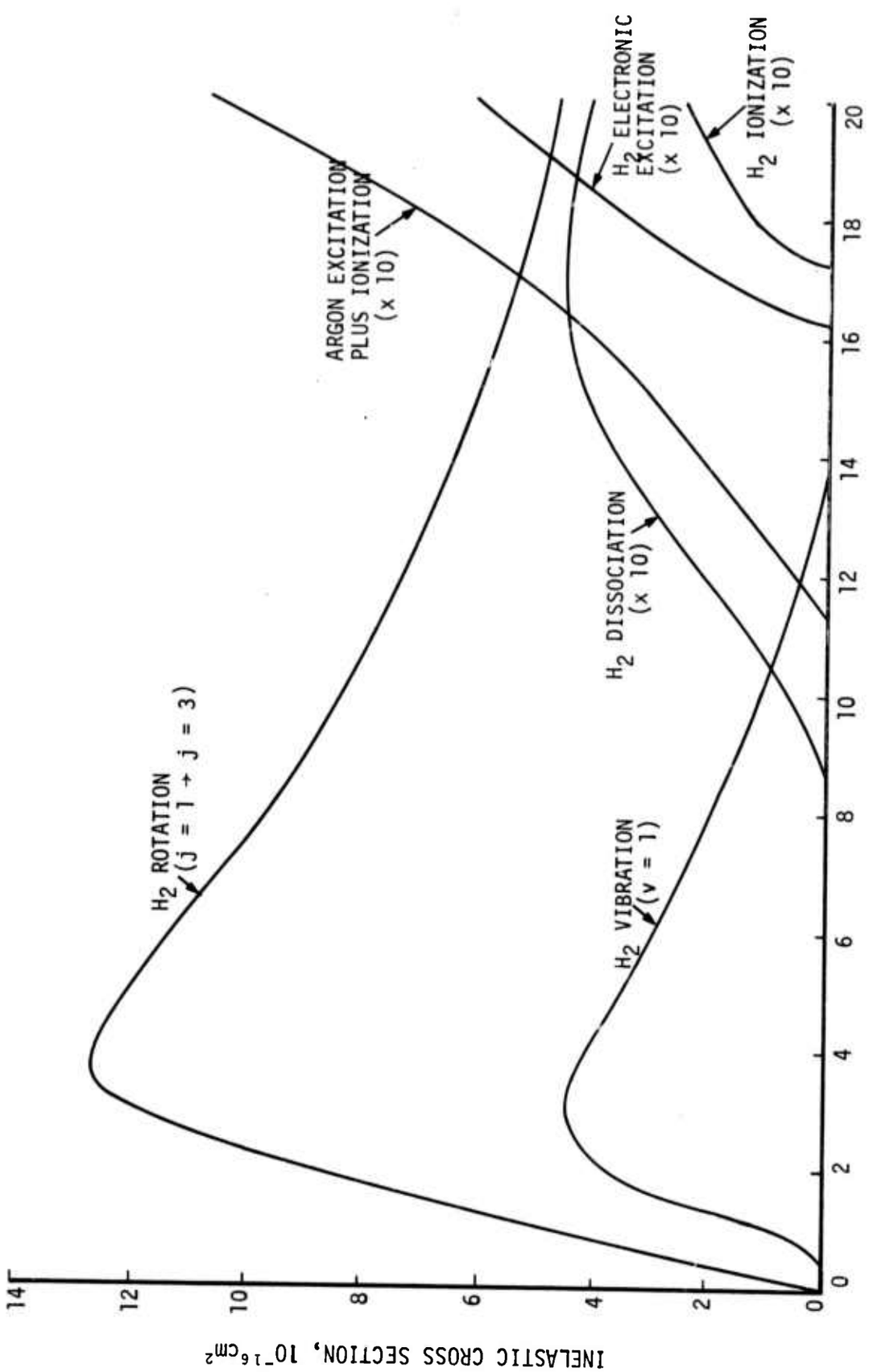

Figure 10. Inelastic Cross Sections for H_2 and Ar

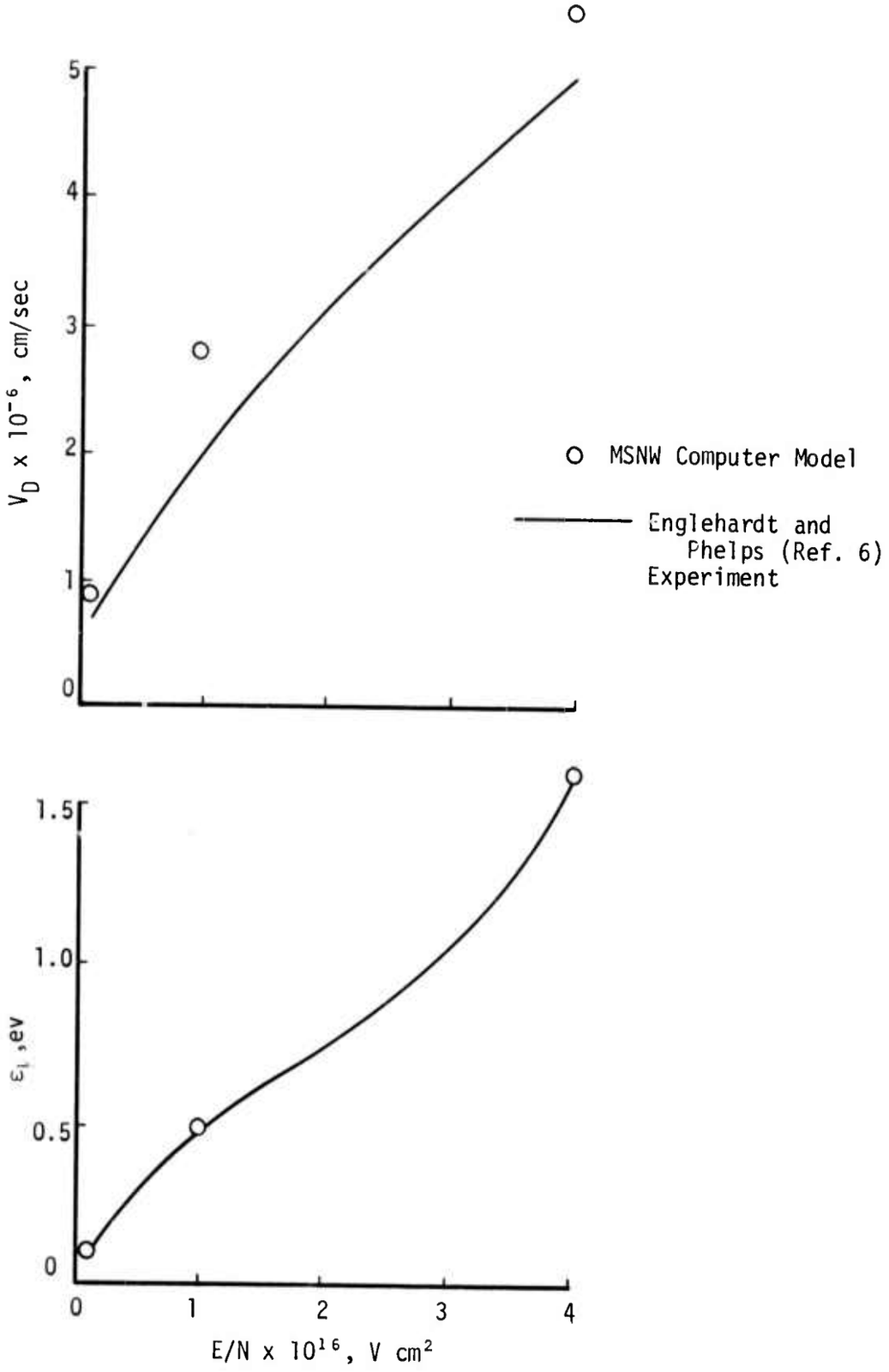

Figure 11. Comparison of Analytical and Experimental Dependence of Electron Transport Properties on E/N for Pure H_2

characteristic electron energy loss of 12 ev is assumed for this process. Good agreement is obtained between computed and measured transport coefficients in pure argon as shown in Figure 12. In Figure 13, the close agreement between our electron distribution function for pure argon with that of Engelhardt and Phelps (Ref. 4) is evident at an E/N of 4×10^{-16} V-cm^2.

It is concluded on the basis of these comparisons that the MSNW computer program for solving the electron Boltzmann equation is working satisfactorily and that the cross sections used are in reasonable agreement with existing experimental data. Thus the program can be applied with confidence to the calculation of energy partitioning in H_2/Ar mixtures.

4.2. Energy Partition in Electric Discharges in H_2/Ar Mixtures

Using the cross sections for electron impact excitation of rotation, vibration, and dissociation of H_2 described in the previous section, the Boltzmann equation was solved for a 10/90 H_2/Ar mixture. The computed drift velocity and characteristic energy are shown in Figure 14. It is seen that the characteristic energy agrees with the experimental results of Engelhardt and Phelps (Ref. 4), whereas the drift velocities are 8% to 20% too high for E/N < 6×10^{-17} V-cm^2.

The fractional power input to the elastic and inelastic processes for a 10% H_2/90% Ar mixture, based on the above Boltzmann solution is shown in Figure 15. It is seen that the optimum power transfer to

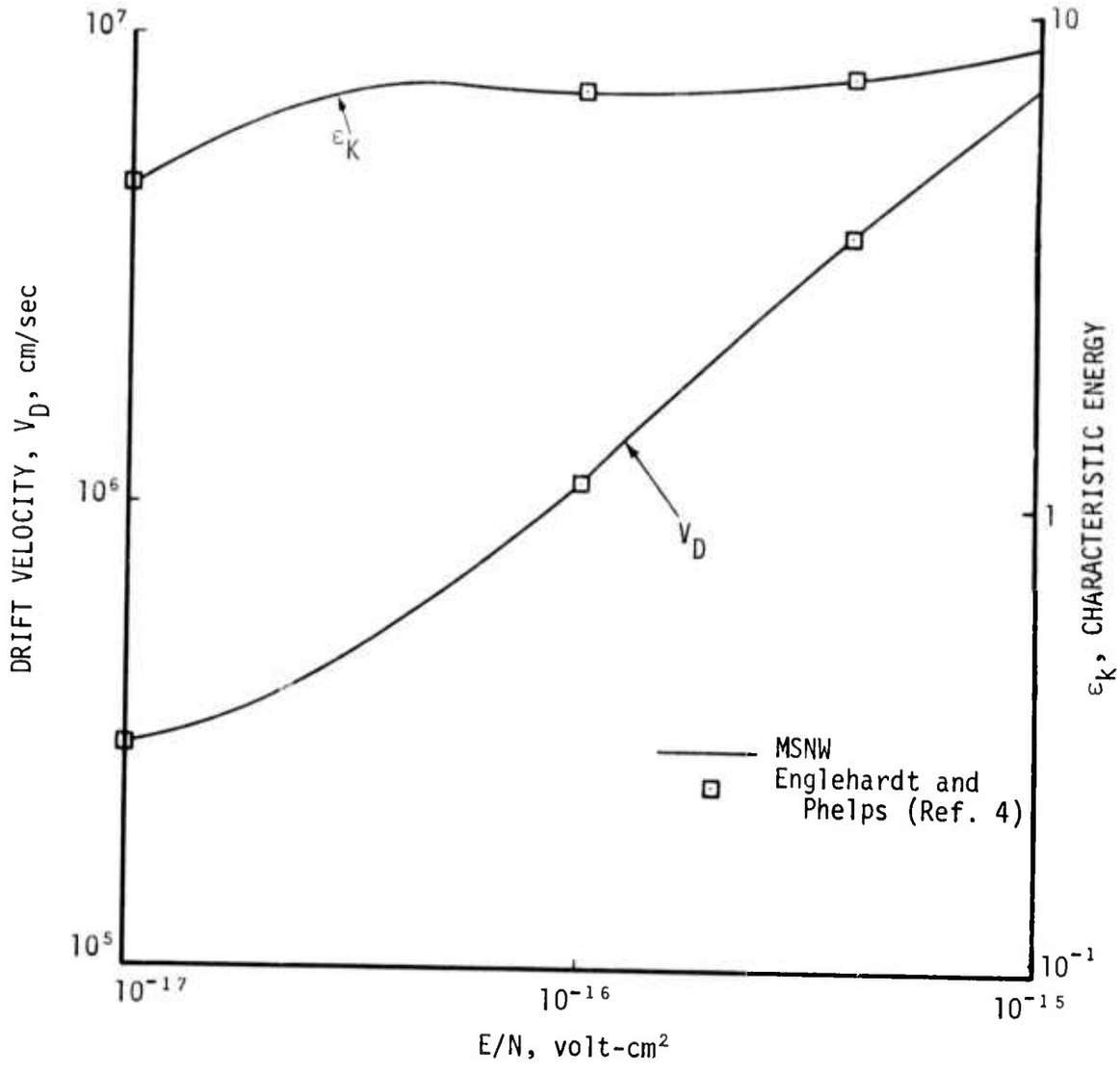

Figure 12. Comparison of Analytical and Experimental Dependence of Electron Transport Properties on E/N for Pure Argon

00031

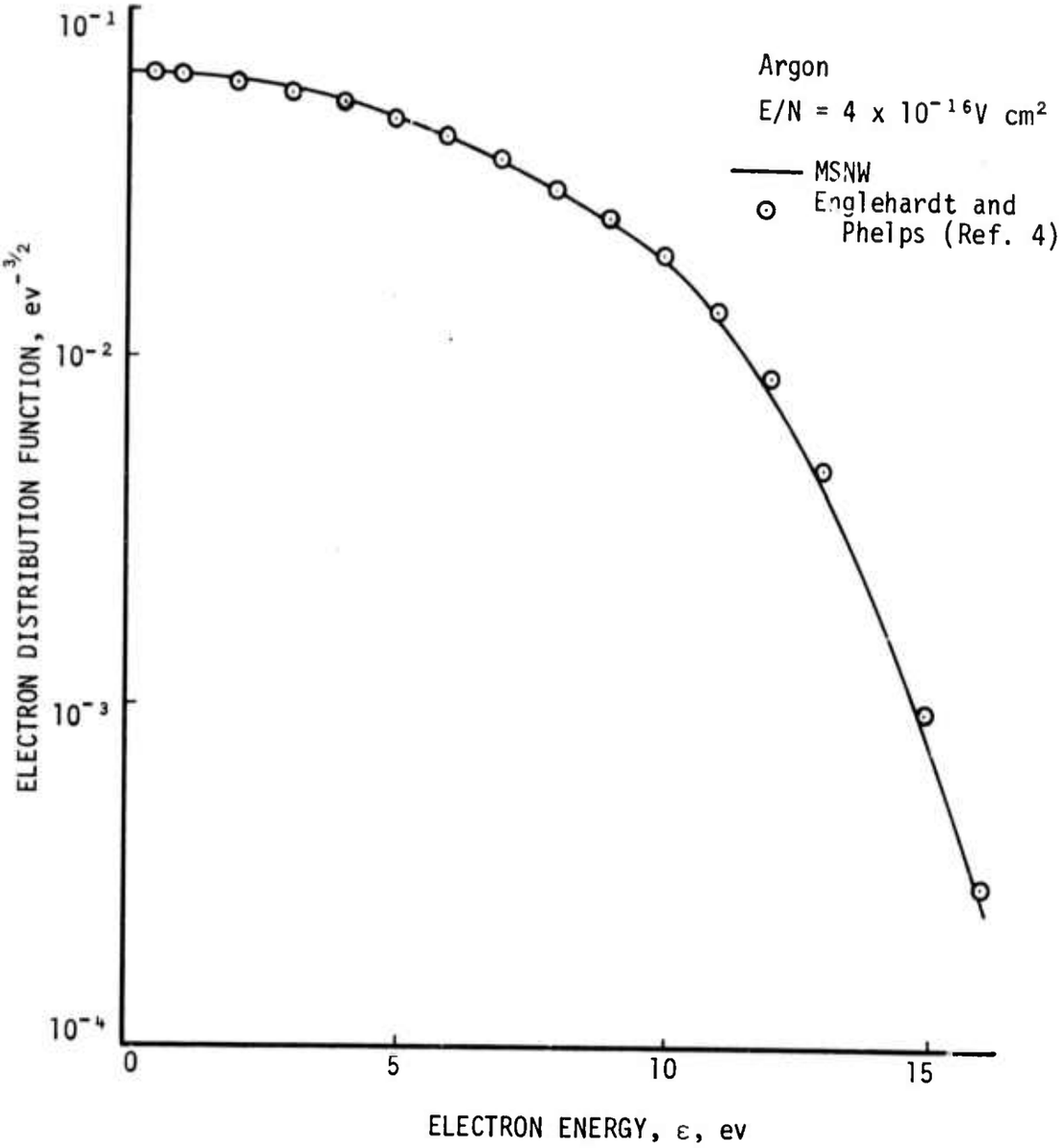

Figure 13. Computed Electron Distribution Function

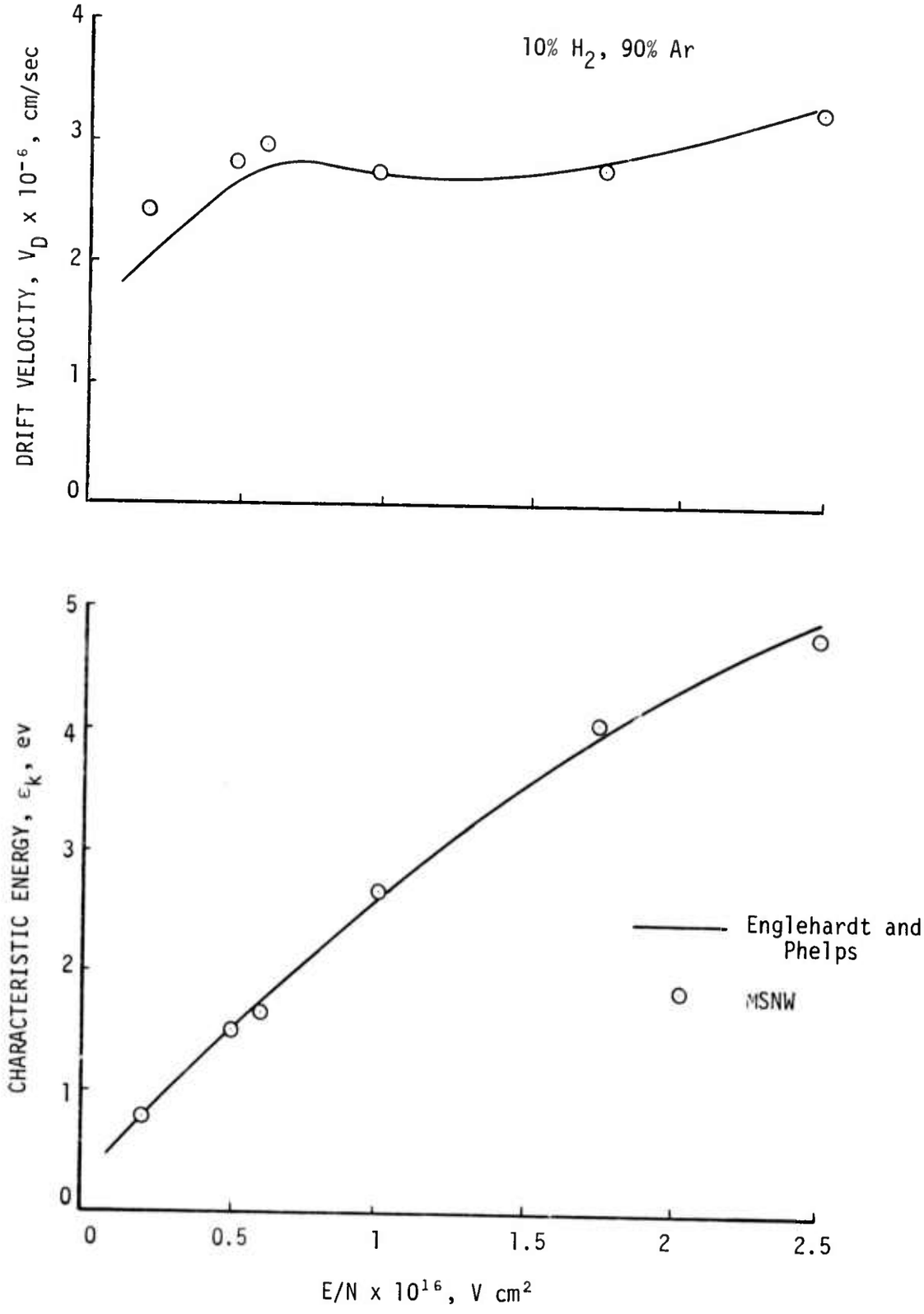

Figure 14. Comparison of Analytical and Experimental Dependence of Electron Transport Properties on E/N for a 10/90 H_2/Ar Mixture

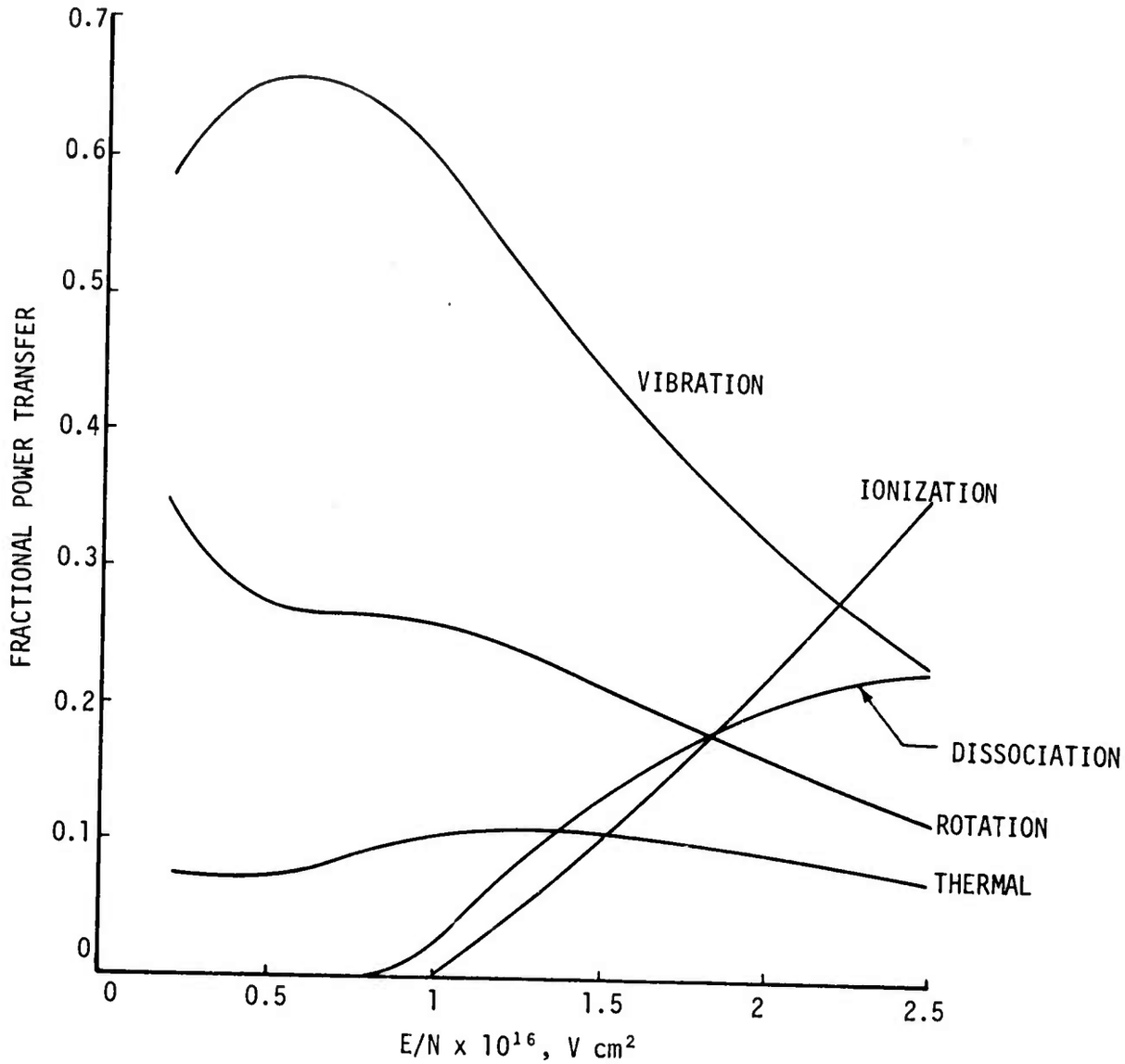

Figure 15. Distribution of Electrical Power in 10/90 Hydrogen/ Argon Mixtures

the vibrational excitation processes occurs for E/N between 0.4 and 0.6×10^{-16} V-cm^2. At these values of E/N, Figure 15 shows that the best electrical efficiency expected for pumping H_2 vibration will be 60-70%, and that rotational heating will be significant (30%). Although the drift velocities used for this calculation are somewhat higher than experiment, the relative amount of power transferred to vibration and rotation is primarily a function of the experimental cross sections and will be relatively insensitive to small errors in the drift velocity.

SECTION V

N_2 LASER

5.1. Kinetics Model

Following the observation at MSNW of repetitive emission pulses on the first and second positive bands of N_2 (Ref. 1), the kinetics of the electronic states of N_2 have been studied in some detail. The current status of this study is summarized here.

An important kinetic process, known as energy pooling, occurs strongly in N_2 according to the reaction

$$N_2(A) + N_2(A) \xrightarrow{k_1} N_2(C) + N_2(X) \qquad (1)$$

The rate constant for this is 2×10^{-11} cm^3/sec according to Stedman and Setser (Ref. 7). The $N_2(X)$ produced is probably vibrationally excited to about V = 6 although this has not yet been verified experimentally. This process has the unique property of removing $N_2(A)$ to produce $N_2(C)$ and, through radiative decay, to produce $N_2(B)$. This process may then provide a collisional inversion mechanism on the first and/or second positive bands of N_2. Such a mechanism could provide a long pulse laser and much greater energy output per liter-atm than is now available in short pulse N_2 lasers.

At the high electronic state populations needed to make good use of Reaction (1), there is significant self-absorption of both the

first and second positive band emission. For this reason it is incorrect to use the optically thin radiative decay time of the C-state or B-state of N_2 as a depletion mechanism in the kinetics analysis. On the other hand, radiative decay cannot be omitted altogether, particularly for the C-state. To avoid the complication of a detailed radiation diffusion model, an effective, reduced, radiative decay time will be used here that is dependent on the optical depth of the band.

This is expressed by

$$N_2(C) \xrightarrow{\tau_1} N_2(B) + h\nu_1 \qquad (2)$$

$$N_2(B) \xrightarrow{\tau_2} N_2(A) + h\nu_2 \qquad (3)$$

In addition to radiative decay of the $N_2(B)$ state, there is an efficient collisional decay mechanism with N_2.

$$N_2(B) + N_2(X) \xrightarrow{k_2} N_2(A) + N_2(X) \qquad (4)$$

Here k_2 is about 1×10^{-11} cm^3/sec into the V = 7 level of $N_2(A)$. Decay down the vibrational ladder of $N_2(A)$ is slower, and is only about 10^{-14} cm^3/sec at the V = 3 and 4 levels (Ref. 8). This latter effect represents a collisional bottleneck that may be overcome by finding an appropriate catalyst. Ethane (C_2H_6) has a rate constant of about 10^{-11} cm^3/sec at V = 3 and 4 and has a sufficiently small quenching rate (3×10^{-13} cm^3/sec) of the electronic energy of $N_2(A)$ (see Ref. 8).

The effect of HF in this regard is not yet known. This collisional process may be important in establishing a two-temperature system to achieve a long lasting inversion on the second positive band of N_2.

An additional collisional process of importance is the removal of vibrational energy from the $N_2(X)$ states produced by Reaction (1).

$$N_2(X)^v + M \rightarrow N_2(X)^{v-1} + M \qquad (5)$$

This may be important in establishing a two-temperature system when using the energy pooling reaction as a pumping mechanism. The $N_2(A)$ to $N_2(X)^{v=0}$ population ratio can be made to be as high as the electron temperature. By making the $N_2(X)^{v=6}$ to $N_2(X)^{v=0}$ population ratio correspond to a vibrational temperature that is much lower than the electron temperature, the reverse of Reaction (1) can be suppressed and the $N_2(C)$ population can be built up to a level that may even exceed the $N_2(A)$ population.

In the overall kinetic model an electron impact pumping term is also needed for each of the electronic states. Detailed cross-section data are currently being gathered and reviewed at MSNW to include in our computer program for solving the Boltzmann equation for the electron distribution function. These pumping terms will be omitted for the present discussion of laser inversion mechanisms.

If we use Reactions (1), (2), and (3), with Reaction (5) to prevent Reaction (1) from going in the reverse direction, we find that the steady state ratio of $N_2(B)$ to $N_2(A)$ is

$$\frac{N_2(B)}{N_2(A)} = k_1 \tau_2 N_2(A) \qquad (6)$$

The spontaneous lifetime, τ_2, is about 5 μsec (Ref. 9) and k_1 is believed to be 2×10^{-11} cm^3/sec (Ref. 7). If self-absorption of the first positive emission produces an effective decay time of 20 μsec, we find that the ratio $N_2(B)/N_2(A)$ exceeds $g_B/g_A (= 2)$ if $N_2(A)$ exceeds $5 \times 10^{15} cm^{-3}$. This is readily possible in high pressure, e-beam stabilized discharges. However, once the population ratio shifts from self-absorption to stimulated emission the effective radiative lifetime suddenly becomes much shorter and superfluorescence will be observed. This effect may be the source of the repetitive pulses that were seen experimentally at MSNW. The optical gain that can be produced is about 1 cm^{-1} if a ΔN of 5×10^{14} cm^{-3} is achieved.

In order to achieve an inversion on the second positive band, it is helpful to add collisional decay of the $N_2(B)$ state by Reaction (4) together with an appropriate catalyst to remove vibrational energy of the $N_2(A)$ state. Then the $N_2(B)$ to $N_2(A)$ population ratio can be collisionally equilibrated at a vibrational temperature which yields a ratio of 0.02 for $T_v \approx 2500°$ K. Then the inversion requirement is

$$\frac{N_2(C)}{N_2(B)} = \frac{k_1 [N_2(A)]^2 \tau_1}{0.02\ N_2(A)} \approx 1 \qquad (7)$$

If τ_1 is taken as 0.5 μsec (10 times the spontaneous lifetime (Ref. 9) to account for self-absorption) the required value of $N_2(A)$ is

2×10^{15} cm^{-3} which is readily achieved. An auxiliary requirement is that the $N_2(A)$ vibrational decay catalyst concentration must be at least $(\tau_1 k_4)^{-1}$ where k_4 is the effective rate constant for descending the A state vibrational ladder. If k_4 is 10^{-11} cm^3/sec, the catalyst must be at least 2×10^{17} cm^{-3} or 7 torr. This is also readily achieved.

In summary, it appears that the energy pooling reaction together with appropriate catalysts may provide an effective mechanism for producing long pulse lasers on the first and second positive bands of N_2.

5.2. N_2 Laser Experiments

An attempt was made to reproduce the previously reported superfluorescent spiking (Ref. 1) on the nitrogen first positive system in $Ar/N_2/HF$ mixtures. Low electron beam currents were used in order to achieve as high an E/N as possible without arcing. However, arcing did occur at an E/N of 1×10^{-16} $V\text{-}cm^2$ and no superfluorescent spikes were observed. Since this value of E/N is too low to produce the required electronic excitation, it was decided to postpone further experiments until a new anode, designed to reduce arcing, could be installed.

5.3. Enhancement of N_2 Laser by SF_6

In an effort to unravel the mechanism leading to the superfluorescent spiking observed in $Ar/N_2/HF$ mixtures (see Ref. 1) the effect of fluorine containing compounds upon the nitrogen first positive laser was investigated in a conventional multipin discharge laser. It was discovered that small concentrations of SF_6 ($\sim$ 1%) in the laser

mix enhanced the laser output by as much as a factor of 1000 on certain lines of the $N_2(B \rightarrow A)$ band. Freon-12 and CCl_4 were also found to enhance the $N_2(B \rightarrow A)$ laser emission, but to a much smaller extent than SF_6. Although the $N_2(C \rightarrow B)$ band could not be made to lase because of current and voltage rise time limitations, the C→B spontaneous emission was doubled when SF_6 was added. However, with the use of electric discharge equipment capable of a very fast rise time, Dr. Colin Willett of the Harry Diamond Laboratory obtained a factor of two to three improvement in the B→A as well as the C→B laser output with the addition of SF_6 to the gas.

The pin laser and its associated electronics used in the studies of SF_6 on the $N_2(B \rightarrow A)$ laser are shown schematically in Figure 16. The discharge tube was constructed from a length of lucite tubing having a bore of 4.5 cm. A 1.4-m length of aluminum rod served as the anode, while the cathode consisted of 110 carbon core resistors (810 Ω) epoxied into holes drilled in the side of the tube. The anode-cathode spacing was 1.0 cm. The CaF_2 Brewster angle windows were mounted onto machined aluminum end pieces which were cemented to the lucite tube. The current pulse had a rise time of approximately 1 μsec and a duration of 1 μsec. The applied voltage ranged from 10 to 20 KV. The optical cavity was formed by two gold-coated spherical mirrors, one with a 5-m and the other with a 3-m radius of curvature. The laser emission was coupled out of the cavity through a 1-mm diameter hole in the 3-m mirror.

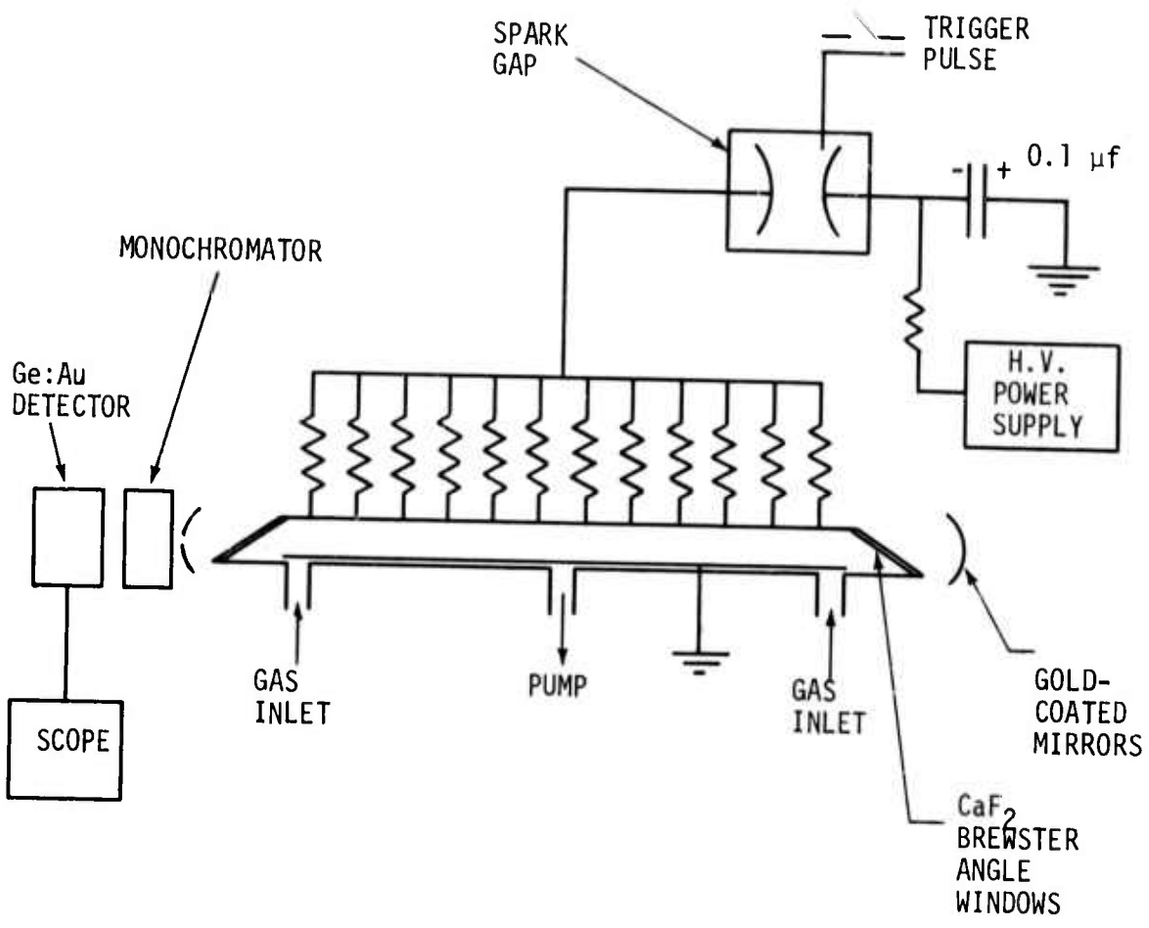

Figure 16. Schematic of the Experimental Arrangement Used to Study the Effect of Electronegative Additives on N_2 First Positive Laser Emission from a Pin Discharge

The spectral line identification was accomplished by passing the emitted light through a Jarrel-Ash 0.25 m Ebert spectrometer, equipped with 6000 Å and 2.1 μm blazed gratings. A Ge:Au detector was used to observe the infrared emission and an RCA C31034 photomultiplier was used for the visible emission. Both detectors had rise times of approximately 0.5 μsec.

A list of the various lines studied with their respective enhancement is presented in Table II. The enhancements refer to the ratio of the laser intensity with a 99% N_2/1% SF_6 gas mixture to that with pure N_2 at a total pressure of 4 torr. The applied voltage was 18 KV. The (2,0) N_2 first positive transition (0.775 μm) was not observed, possibly because the reflectivity of the gold mirrors drops below 90% at 8000 Å.

The addition of SF_6 significantly reduced the threshold for lasing, and thus the enhancements could be exaggerated by operating the laser close to the threshold voltage. In the case of CCl_4, the enhancement was only observable when the laser was run at low voltages close to threshold. In the case of SF_6, the optimum concentration was independent of pressure for total pressures from about 4 to 20 torr.

Table II

Enhancement of $N_2(B \rightarrow A)$ Laser Lines by SF_6

$N_2(B \rightarrow A)$ Transition	Wavelength(μm)	SF_6 Enhancement
(0,0)	1.048	3
(0,1)	1.231	10^3
(1,0)	0.888	10
(2,1)	0.870	10^3

In an effort to elucidate the role of SF_6 in enhancing the N_2 first positive laser, an attempt was made to measure a change in the discharge current and voltage. A Rogowski coil was used to monitor the current and a 1000:1 (6 KΩ: 6Ω) voltage divider was used to measure the discharge voltage at several pins. However, no discernible difference could be detected with SF_6. The discharge voltage was found to be approximately 800 V/cm corresponding to an E/N of 60×10^{-16} V-cm^2.

It was possible, however, to see a change in the discharge characteristics visually. The luminous core from each pin discharge constricted noticeably when SF_6 was added to the gas mixture.

Although the discharge voltage and current measurements did not reveal any overall differences with and without SF_6, the addition of SF_6 may significantly alter the electrical properties of the discharge. SF_6 is known to have a large attachment cross section for low energy electrons (Ref. 10). Thus the addition of SF_6 to the laser gas will remove low energy electrons which have a small cross section for pumping the nitrogen B and C states. This same explanation would also hold for CCl_4 and freon-12 because they too have large attachment cross sections for low energy electrons (Ref. 10). The removal of these low energy electrons and constriction of the discharge volume by SF_6 could lead to a shift of the electron distribution function to higher energies even though the observed voltage changed very little. In addition, low energy electrons are known to undergo superelastic collisions with excited molecular electronic states, hence their removal may reduce one of the deactivation losses.

SECTION VI

SUMMARY OF RESULTS

1. Laser oscillation in electrically excited Ar/HF and $Ar/H_2/HF$ mixtures has been achieved using a high current, electron-beam-stabilized electric discharge. DF laser action has not been observed to date, and experiments are being planned to better purify the test gases used.

2. HF lasing has also been observed in N_2/HF and $Ar/N_2/HF$ mixtures. Probe laser measurements of the HF vibrational decay rate will be made to determine the pumping mechanism in these mixtures.

3. Preliminary evidence indicates that V-V transfer is the principal pumping mechanism in $Ar/H_2/HF$ mixtures. Decay rates of HF (v = 1, 2) will be measured to verify this mechanism and to obtain V-V and V-T kinetic information on the upper HF levels.

4. Characterization of the plasma diode electron beam source has shown that e-beam currents of the order of 100 ma/cm^2 can be obtained. Current density profiles of the 5-tube device need to be measured since nonuniformity is suspected. Current inhomogeneities could lead to regions of significant absorption in the optical path. Variation of the laser output with e-beam current will be studied since it is expected that more e-beam current will lead to higher HF output, due to increased excitation rates.

5. Boltzmann calculations of the fractional power transfer for electrical excitation in argon/hydrogen mixtures have shown that above an E/N of 1×10^{-16} $V\text{-}cm^2$ significant H_2 dissociation occurs. Hence, increased H_2 vibrational pumping rates can only be achieved by further

increasing the e-beam current. In addition, simultaneous rotational and vibrational excitation of the H_2 results in an inherent limitation of 60 - 70 percent on the overall electrical efficiency.

6. Gases with large electron attachment cross sections, at low electron energies, can increase the output of various N_2 infrared laser lines by factors of 10 to 1000. Experiments performed at Harry Diamond Laboratories by Dr. C. Willett have shown that the total output of a fast pulse N_2 laser can be increased by factors of two or three in both the infrared and the ultraviolet.

7. Kinetic modeling of the nitrogen lasers has shown that the $N_2(A)$ state energy-pooling reaction coupled with appropriate catalysts for relaxing N_2 electronic and vibrational excitation may provide an effective mechanism for long pulse lasers operating on the first and second positive system. Experiments to test these hypotheses and to unravel the mechanism responsible for the previously observed super-fluorescent spiking are currently being planned.

REFERENCES

1. S. R. Byron, "Electron Beam Molecular Lasers," Semi-Annual Technical Report, MSNW Report No. 72-105-1, November 1972.

2. B. B. O'Brien, Jr., Appl. Phys. Lett. 22, 503 (1973).

3. S. N. Suchard, Appl. Phys. Lett. 23, 68 (1973).

4. A. G. Englehardt and A. V. Phelps, Phys. Rev. 133, A375 (1964).

5. F. Linder and H. Schmidt, Zeitschrift für Naturfoschung, 26A, 1603 (1971).

6. A. G. Englehardt and A. V. Phelps, Phys. Rev. 131, 2115 (1963).

7. D. H. Stedman and D. W. Setser, J. Chem. Phys. 50, 2256 (1969).

8. J. W. Dreyer and D. Perner, J. Chem. Phys. 58, 1195 (1973).

9. R. Anderson, Atomic Data 3, 227 (1971).

10. D. Spence and G. J. Schulz, J. Chem. Phys. 58, 1800 (1973).